INC Technical Report

Institute for Neural Computation

University of California, San Diego

ID: INC-08-001

Date: October 30, 2008

Title: Independent Component Analysis of Optical Recordings from *Tritonia* Swimming Neurons

Authors: Glen D. Brown[a,b], Satoshi Yamada[a], Michio Nakashima[a], Caroline Moore-Kochlacs[b], Terrence J. Sejnowski[b,c], Satoru Shionoa[a]

[a] Advanced Technology R&D Center, Mitsubishi Electric Corporation, Amagasaki, Japan
[b] Howard Hughes Medical Institute, Computational Neurobiology Laboratory, The Salk Institute for Biological Studies, La Jolla, CA
[c] Division of Biological Sciences, University of California, San Diego, La Jolla, CA

Independent Component Analysis of Optical Recordings from *Tritonia* Swimming Neurons

Glen D. Brown[a,b], Satoshi Yamada[a], Michio Nakashima[a], Caroline Moore-Kochlacs[*,b], Terrence J. Sejnowski[**,b,c], Satoru Shiono[a]

[a] *Advanced Technology R&D Center, Mitsubishi Electric Corporation, Amagasaki, Japan*
[b] *Howard Hughes Medical Institute, Computational Neurobiology Laboratory, The Salk Institute for Biological Studies, La Jolla, CA 92037*
[c] *Division of Biological Sciences, University of California, San Diego, La Jolla, CA 93093*

Abstract

Independent Component Analysis (ICA) blindly separates mixtures of signals into individual components. Here we used ICA to isolate spike trains from individual neurons recorded optically in the *Tritonia diomedea* isolated brain. ICA removed several types of artifacts, allowed us to view an approximation of the membrane potential as opposed to the usual raster diagram, and provided an automated method for viewing the locations of individual neurons or groups of neurons in the brain. Action potentials from as many as 132 individual neurons were identified in a single recording. During fictive swimming we found almost twice as many candidate swimming-network neurons as might be expected from current models, including neurons with previously unrecognized firing patterns. In addition, novel forms of coordinated population activity appeared in several recordings after the end of fictive swimming. Thus, ICA provides a powerful way to explore the activity of neuronal populations, for example during multiple fictive behavior patterns in the same preparation.

Key words: Independent Component Analysis, central pattern generator, rhythmic behavior

1. Introduction

Identifying the network of neurons and synapses associated with swimming in the seaslug *Tritonia* has been the goal of neurophysiological studies for almost four decades. The swimming network has been explored with intracellular and extracellular recordings in a variety of reduced preparations, including the isolated brain where swimming neurons can be induced to fire rhythmic bursts of action potentials that closely resemble those recorded during swimming in semi-intact preparations [2, 3, 4, 5, 6]. These studies of fictive swimming have identified a few dozen neurons involved in the *Tritonia* swimming network.

Optical recording could, in principle, allow us to determine the completeness of these studies and to find as yet unidentified neurons in the network. For example, Briggman KL et al. [7] recently used optical recordings from the medicinal leech to identify a neuron involved in the decision-making

[*] Principal corresponding author
[**] Corresponding author
Email addresses: glen@salk.edu (Glen D. Brown), yamada.satoshi@wrc.melco.co.jp (Satoshi Yamada), naka@cs.kusa.ac.jp (Michio Nakashima), carolmk@salk.edu (Caroline Moore-Kochlacs), terry@salk.edu (Terrence J. Sejnowski), shiono.satoru@wrc.melco.co.jp (Satoru Shiono)

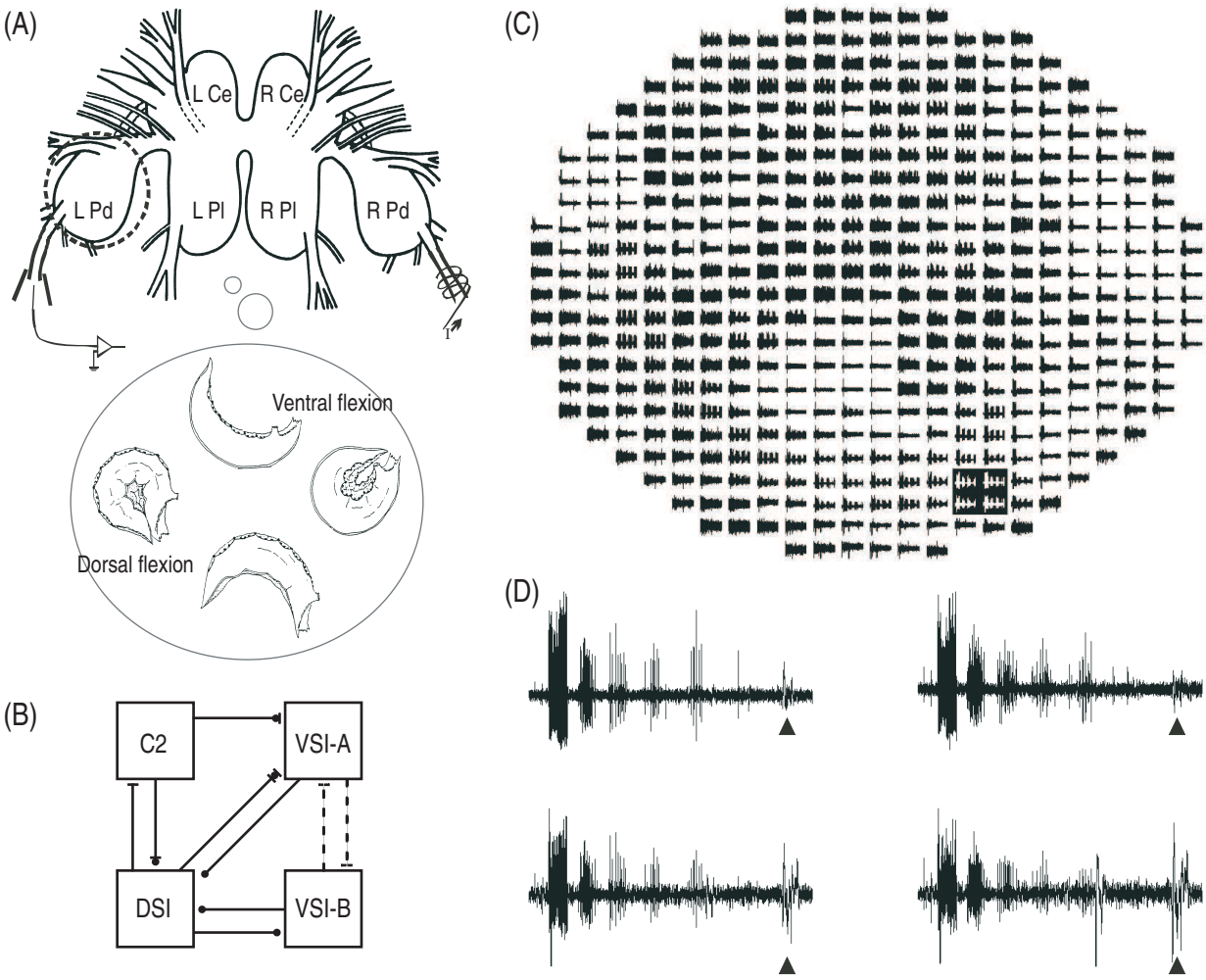

Figure 1: Fictive swimming with photodiode array.
(A) Fictive swimming in the isolated brain. A sequence of ventral and dorsal flexions, clockwise around the inset, characterize the natural swim behavior. The Tritonia isolated brain preparation contains paired pedal (Pd) and cerebral (Ce)-pleural (Pl) ganglion (abbreviated as CP). (Right and left are labeled by R and L, respectively.) Cell somata form the outer shell of the ganglia while axons and dendrites synapse with one another in the interior. Ventral and dorsal flexion neurons, which activate swimming musculature, are located in the pedal ganglion while swimming interneurons (schematic, part B) have been found in the cerebral-pleural ganglion. Brief current pulses (I) applied to a pedal nerve root activated the fictive swimming pattern (see also Fig. 2) while suction electrode recordings from the other pedal nerve root recorded action potentials from the axons. The dashed line circle shows the approximate field of view for pedal ganglion recordings.
(B) Schematic of the swimming interneuron network. During swimming, DSI, VSI, C2, and other neurons form a pattern-generating network that oscillates with a period of about seven seconds. VSI-B and other unidentified neurons excite the downstream ventral and dorsal flexion neurons (not shown). Getting PA [1] modeled the interactions between these Tritonia-swimming interneurons.
(C) Photodiode array. After the brain was stained with a voltage-sensitive absorbance dye and placed under a microscope, a 448-element photodiode detector array recorded changes in light absorbance due to fluctuations in the membrane voltage of underlying neurons. Raw data is displayed with the shape of the electrode array preserved (each detector, y-axis proportional to transmitted light, x-axis 45 s total). Some action-potential bursts may be seen even at this low magnification.
(D) Raw data. A blow-up of four channels marked with a negative image in (C) shows raw data at a higher magnification. Subsequent analysis determined that these diode channels contain action potentials from three neurons and also several recording artifacts. Triangular arrows show the temporal location of one artifact.

process. In the present study we use optical recording together with ICA, a powerful new signal-processing technique, to estimate the number of neurons in the *Tritonia* swimming network, to get a more global view of how these neurons contribute to the swimming behavior, and to observe the non-swimming activity of swimming-network neurons.

Tritonia swimming consists of up to 20 cycles of ventral and dorsal whole-body flexions (Figure 1A). An initial ventral flexion lifts the slug into prevailing currents, and subsequent dorsal and ventral flexions tend to keep the animal aloft as it bounces along the ocean floor. One ventral/dorsal cycle lasts about seven seconds. Flexion musclulature is activated, either directly or indirectly via a peripheral nerve net [8], by ventral and dorsal flexion neurons (VFN and DFN) in the pedal ganglion [4, 8, 9, 10]. *Tritonia* flexion neurons do not synapse with one another directly, perhaps because they must remain flexible enough to produce behaviors other than swimming [5, 9]. Instead, VFN and DFN receive excitatory and inhibitory synaptic inputs from a population of swimming interneurons located in the cerebral-pleural ganglion [6].

The first swimming interneuron discovered, cerebral cell 2 (C2), appears on the dorsal surface of each cerebral ganglion [5, 11]. Depolarizing a single C2 with an intracellular electrode to fire action potentials can trigger swimming, and hyperpolarizing both C2 can prevent swimming. The C2 fire a single burst of action potentials per cycle of swimming (known as fictive swimming in reduced preparations) as do all other *Tritonia* swimming interneurons reported so far. Closer to the input side of the network, the dorsal ramp interneuron (DRI), can also start or prevent the fictive pattern [12]. Two other groups of interneurons, Ventral and Dorsal Swimming Interneurons (VSI and DSI), form a pattern-generating network with C2, DRI, and probably other neurons as well [5, 13] (Fig. 1B). The synaptic connections between these neurons tend to have multiple components; for example, C2 synapses can have at least four effects on the membrane potential of a single post-synaptic neuron [14, 15].

2. Results

Recordings were made from both the dorsal and ventral surfaces of the pedal ganglion and the cerebral-pleural ganglion, in slightly different planes of focus (see Materials and Methods). The results and the figures will be organized according to the ganglion recorded. This corresponded approximately to the class of neurons, which tend to be clustered in different parts of the ganglia.

2.1. Pedal Ganglion

In 64 isolated brain preparations, we made 70 recordings from the dorsal (N=60) and ventral (N=10) surfaces of the pedal ganglion that appeared to contain action potential activity from at least one neuron. Due to recording artifacts or low signal-to-noise ratio in many preparations, only 13 recordings (10 dorsal and 3 ventral) were analyzed further. These selected recordings are the best yet obtained from this preparation and provided high quality recordings from a large number of neurons. In the two dorsal-side recordings with the greatest number of individual neurons, we found 132 and 111 spike trains. These two recordings also contained the most bursting neurons, 64 (Fig. 2A,C) and 52 respectively. The best ventral-side recording of the pedal ganglion had 31 distinct spike trains including 22 swimming-network neurons (Fig. 2B, Fig. 4).

Figure 2A,C shows selected neurons from our best dorsal-side pedal ganglion recording during a fictive swimming episode (neurons classified after Hume RI et al, 1982 [10]). Many pedal neurons fired a burst of action potentials during the nerve stimulus. The swimming pattern began after termination of the nerve stimulus with a burst in the VFN. VFN and DFN then fired alternating bursts until the pattern terminated after a burst in the DFN.

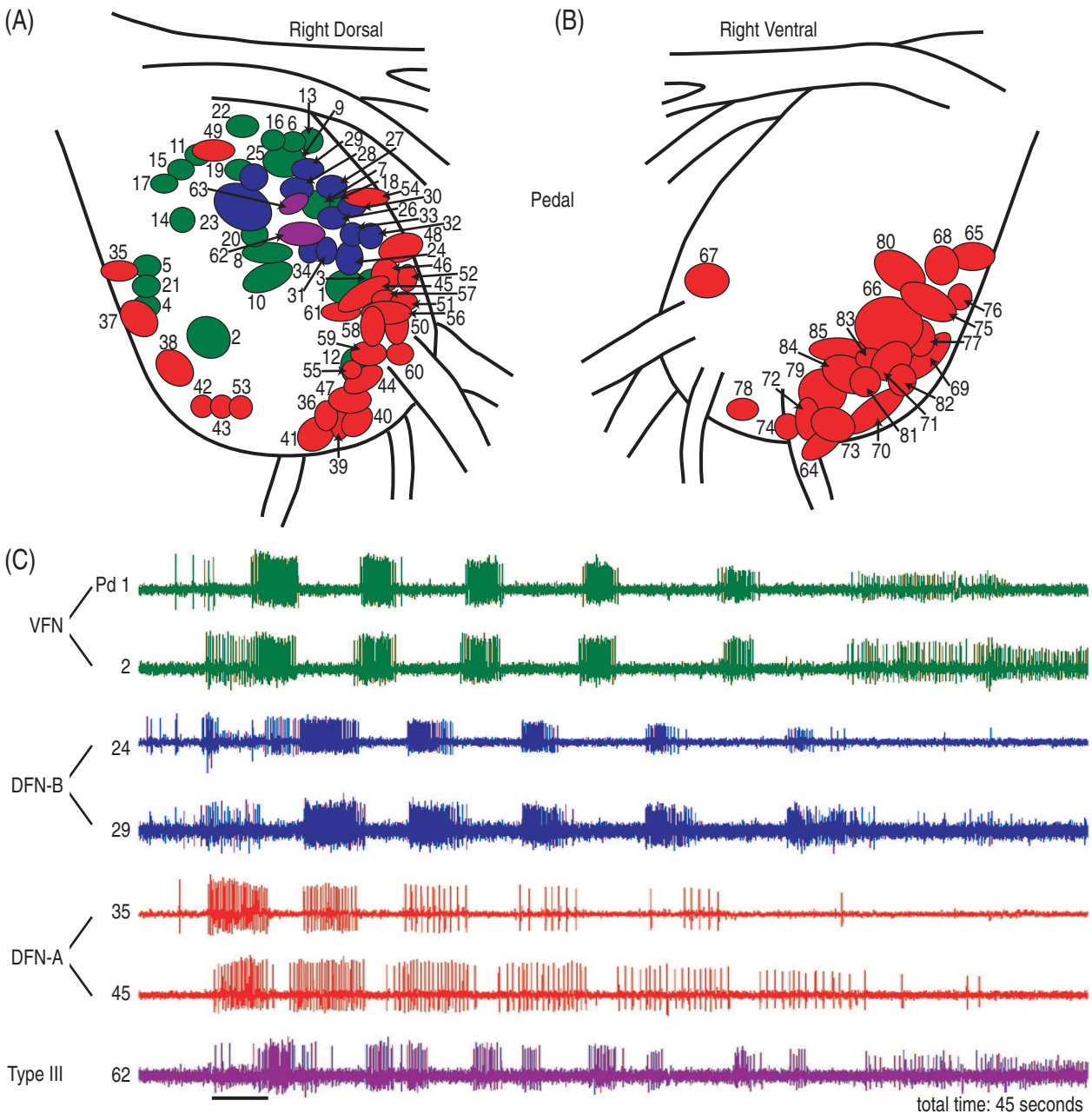

Figure 2: Pedal ganglion efferents.
(A) Dorsal side. Place maps for each neuron were classified and colored according to their corresponding spike trains and combined to form topographic maps. Type A dorsal flexion neurons (DFN-A) are shown here and elsewhere in red, type B dorsal flexion neurons (DFN-B) in blue, ventral flexion neurons (VFN) in green, and type III neurons in purple. VFN and DFN-B clustered on the rostral half of the ganglion.
(B) Ventral side. Place maps reveal the topography of the DFN-A on the ventral side of the ganglion. On both the dorsal and ventral surfaces, DFN-A clustered on the medial, caudal, and lateral parts of the ganglion.
(C) Dorsal efferent activity. Following a brief electrical stimulus (bar, lower left, here and throughout), which elicits firing in some neurons, fictive swimming begins with a burst of action potentials in the VFN and ends after a DFN burst. This activity parallels the swimming behavior, which begins with a ventral flexion and ends after a dorsal flexion (Fig. 1).

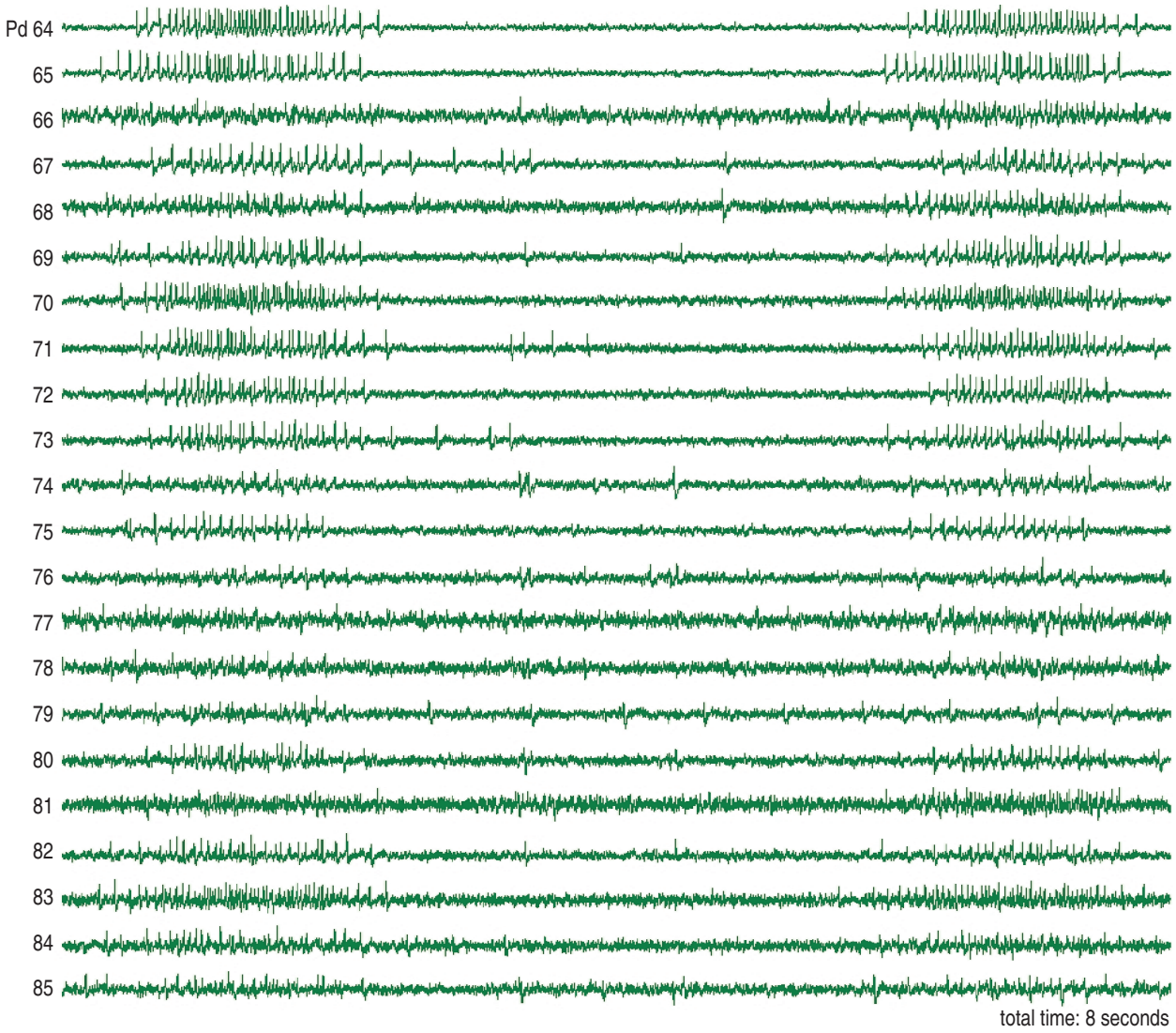

Figure 3: VFN
The second and third bursts of action potentials from 22 VFN recorded on the dorsal side of the pedal ganglion. This doubles the estimate for the number of VFN in one pedal ganglion (see Table 1). A range of firing rates during bursting may be seen, but all VFN had the same phase. Some neurons fired action potentials at a very low frequency between bursts.

VFN appeared in a total of nine dorsal-side recordings (6.9 $\pm$ 7.9), but three preparations contained only one VFN each. There were 22 (Fig. 2A, locations in dark green, spike trains in Fig. 3), 16, and 7 VFN in the three best preparations. If the best recording represents the population, then this approximately doubles the previous estimate of VFN active during fictive swimming (Table 1).

DFN were split into DFN-B and DFN-A depending whether or not, respectively, they phase lock to other swimming network neurons [10]. DFN-B appeared in 6 recordings from the dorsal side of the ganglion, including 12 (Fig. 2A, blue), 6, and 4 DFN-B in the three best recordings. Hume RI et al [10] found at least 20 DFN-B so their estimate may be more accurate. In future studies it may be possible to orient the ganglion with the rostral end tilted upward to better record

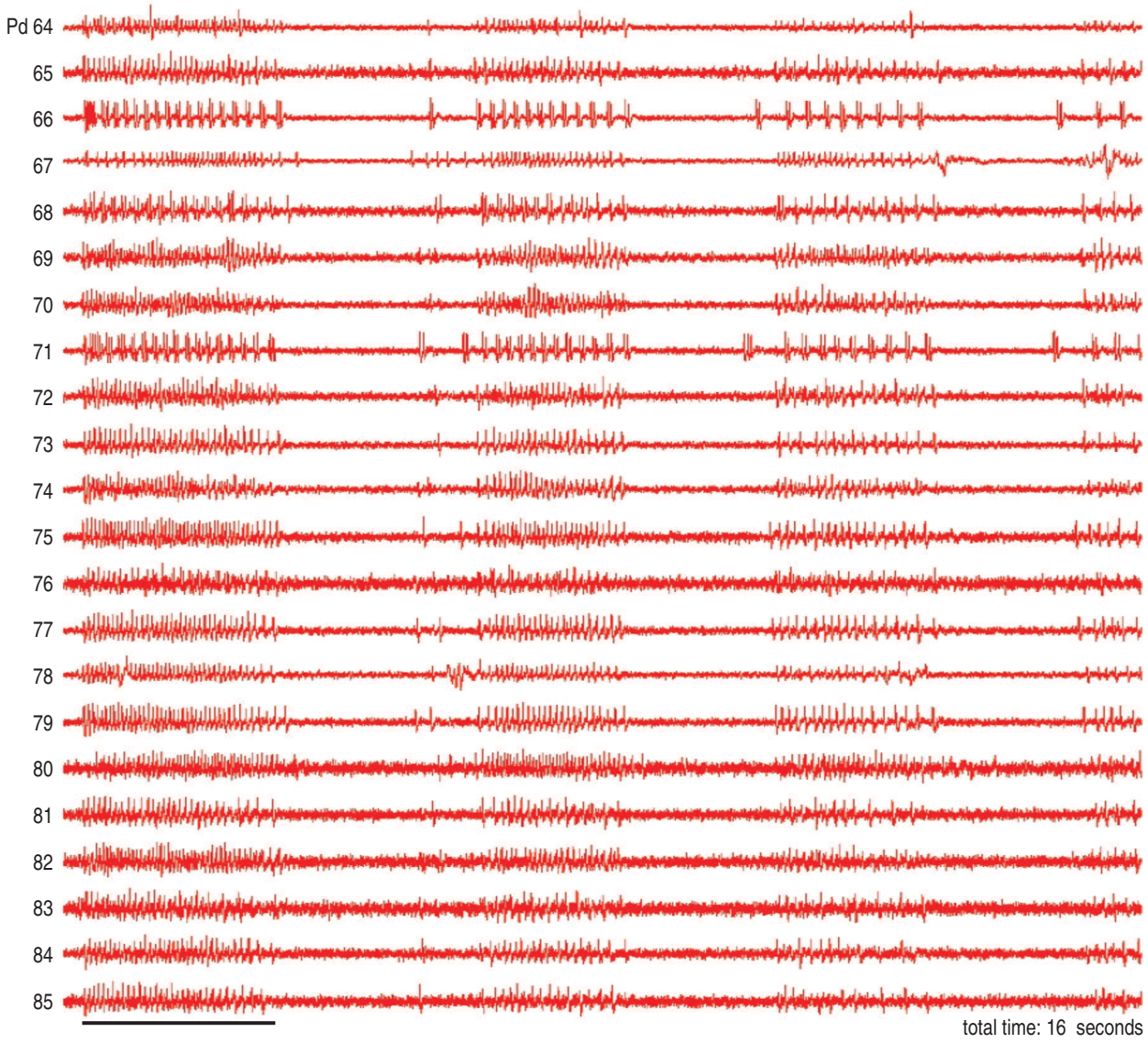

Figure 4: DFN-A
Action potential bursts from 22 DFN-A appeared in this ventral-side recording of the pedal ganglion (see Fig. 2B for topographic map). Burst initiation and termination times were remarkably similar across the population. Several DFN-A consistently fired doublets (Pd 66, 68, and 71) perhaps due to depolarizing after potentials [16]. Spikes were usually about the same shape in a single DFN-A, but fluctuations were observed in some neurons (e.g. spike height in Pd 69, 70, and 74). Note that the burst of firing in these neurons during the stimulus are not part of a swim cycle (see also Fig. 2)

DFN-B.

All 13 pedal ganglion recordings contained DFN-A. On the dorsal side, an average of about 16 DFN-A appeared in 10 preparations, including 27, 27, and 26 in the three best recordings. On the ventral side we counted 22 DFN-A in two preparations (one example in Fig. 2B) and 18 in a third. Neither DFN-B nor VFN appeared on the ventral side of the ganglion in these recordings (but see below and Fig. 5). Figure 4 shows DFN-A spike trains during the first three and half cycles of fictive swimming.

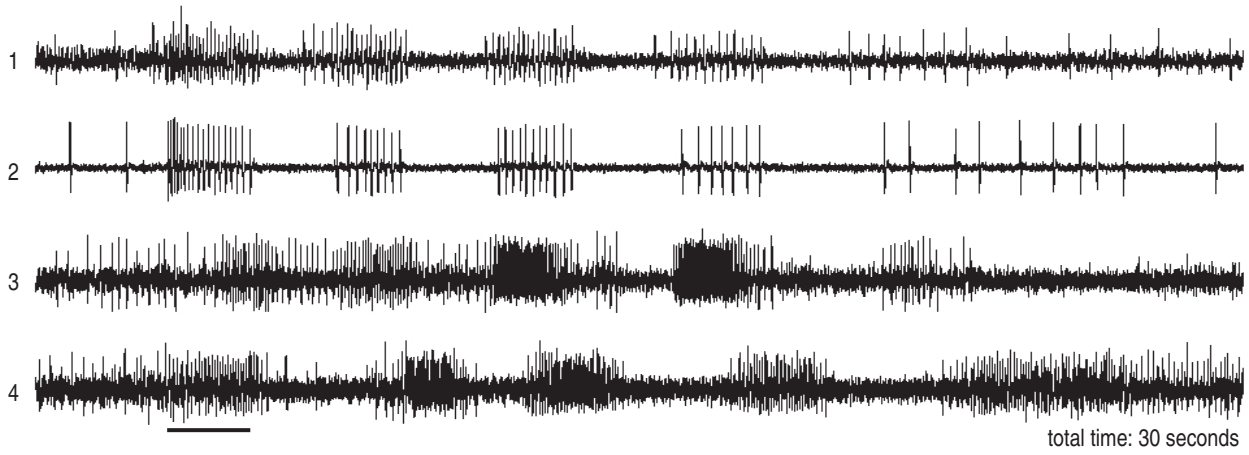

Figure 5: New pedal ganglion neurons.
DFN-A appeared in this recording of the ventral pedal ganglion (recordings 1 and 2) as expected. Neuron 3 also appears to be a DFN of sorts, but the bursts at the end of fictive swimming were stronger than those at the beginning, contrary to the prevailing pattern. Neuron 4 fires something like a VFN but did not fire during the first cycle of fictive swimming. Another new type of pedal neuron may be seen in Figure 8 (Pd 90).

Hume RI et al. [10] found less than 10 DFN on the ventral side of the ganglion and estimated the total DFN pool to be about 50 including 20 DFN-B. We added DFN-A from dorsal and ventral recordings to estimate the number of DFN-A in the pedal ganglion because we appeared to be recording from separate populations in the two cases. Adding the dorsal and ventral sides, we raise the estimated lower bound for the number of DFN-A to 49 (Table 1). For all other neuron types, we estimated the size of the population from the single recording with the most neurons of that type (Table 1).

Two other groups of swimming network neurons with unknown function have been identified in the pedal ganglion. Type III neurons fire during both the VFN and DFN bursts while Type IV neurons fire when Type III neurons are silent [4, 10]. Neurons that fired more than one burst of action potentials per cycle of fictive swimming occurred in only 3 of 13 pedal-ganglion recordings (6 neurons total). Figure 2 shows a candidate Type III neuron in purple (Pd 62), though no double burst occurred on the first cycle in this case. In all six cases, one of the two bursts per cycle had more spikes and a higher firing frequency than the other. In two of the six neurons, no double bursts occurred after the first cycle of fictive swimming.

We also made a few partial recordings of the pedal ganglion while recording primarily from the cerebral-pleural ganglion. On both the dorsal (N=3) and ventral (N=3) sides, we found a different subset of neurons than when we focused on the top surface of the pedal ganglion itself. On the dorsal side, we found a higher percentage of Type III and IV neurons suggesting that these populations extend toward the medial surface of the ganglion. On the ventral surface we found primarily DFN-A, but also observed patterns of activity that do not match any previously reported (Fig. 5).

2.2. Cerebral-Pleural Ganglion

Sixty-five recordings contained all or part of at least one cerebral-pleural ganglion. Nineteen had at least one neuron that fired discreet bursts of action potentials during swimming. Of these, 13 (9 dorsal and 4 ventral) were judged suitable for further analysis.

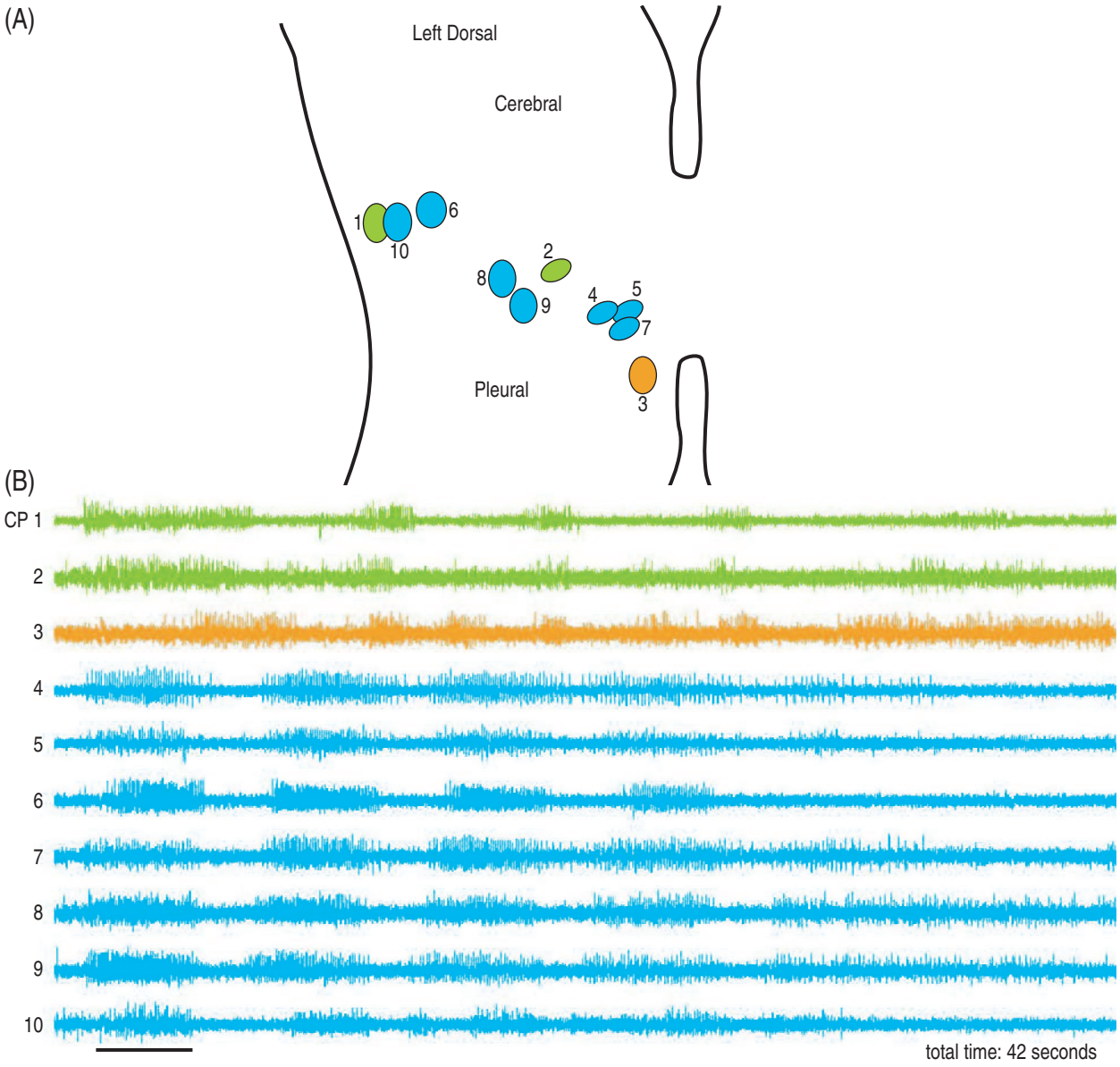

Figure 6: Left dorsal cerebral-pleural ganglion.
Seven DPN (light blue, CP 4-10) are clustered near the fused border between the cerebral-pleural ganglion. Earlier studies have described only four DPN in this region of the brain [5]. CP 6 is a C2 candidate. CP 8, 9 are DSI candidates. Two VPN are shown in light green (CP 1,2). Neither VPN was in the correct position for a candidate VSI-A. CP 3 (orange) is another interesting bursting neuron.

We classified cerebral-pleural ganglion neurons broadly as dorsal phase neurons (DPN) if they fired one burst of action potentials per cycle of fictive swimming and their bursts substantially overlapped with DSI-candidate or DFN bursts. Bursting neurons were classified as ventral phase (VPN) if their bursts did not substantially overlap with DSI-candidate or DFN bursts. DSI, C2, and DRI would all be classified as DPN according to this scheme while VSI would be considered a VPN.

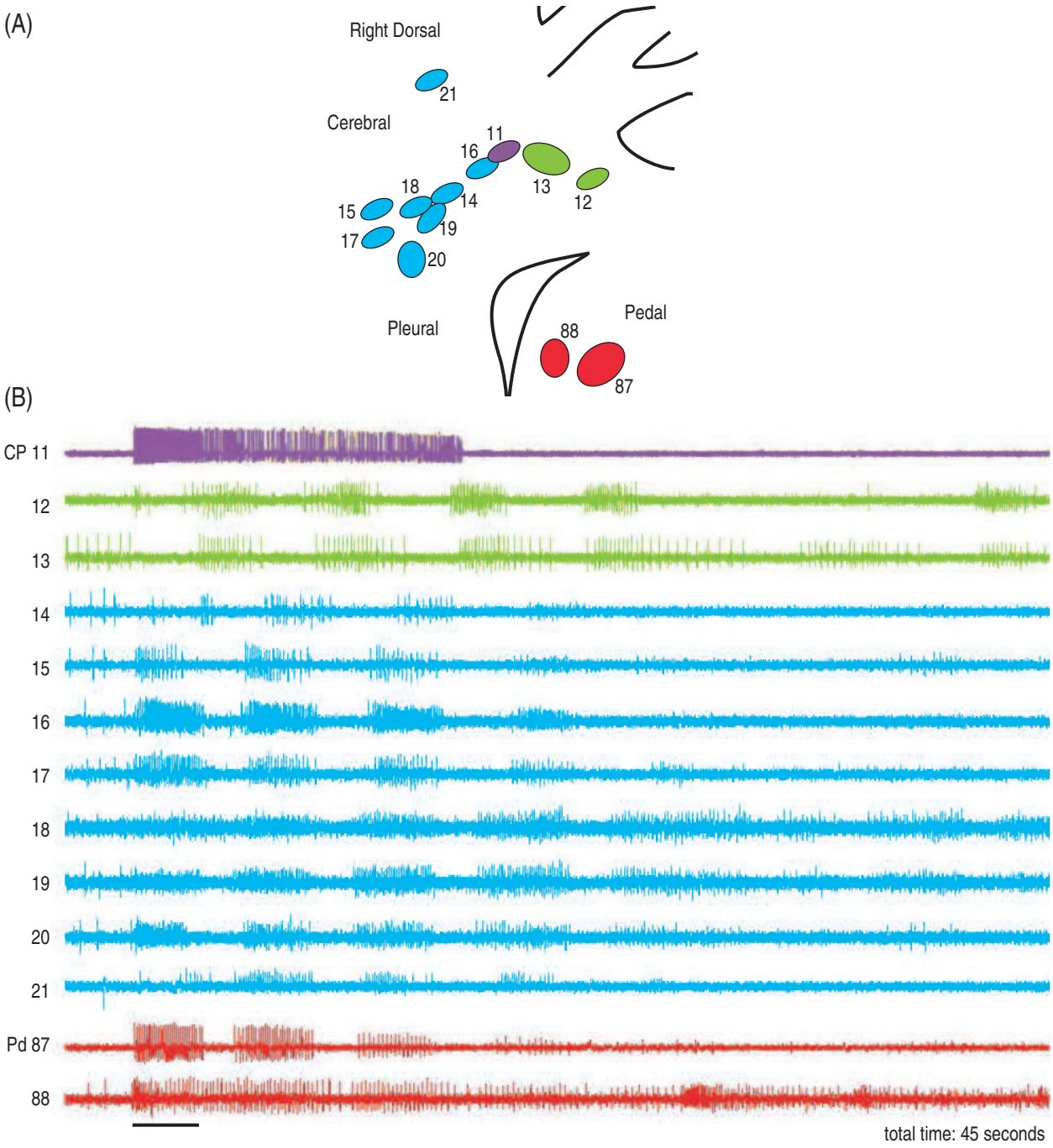

Figure 7: Right dorsal cerebral-pleural ganglion.
The eight DPN (light blue, CP 14-21) seen in this recording are also clustered in the cerebral ganglion near the cerebral-pleural border. DSI candidates (CP 16- 20) fired weakly before the nerve stimulus, burst strongly during the nerve stimulus and fictive pattern, and fired at an elevated rate after fictive swimming terminated. CP 21 is a C2 candidate. Two VPN appeared in the rostral-lateral part of the cerebral ganglion (light green, CP 12, 13), neither was a VSI-A candidate. Another neuron fired a single burst of action potentials during the first two cycles of the fictive pattern (purple, CP 11). One VPN (CP 12) and one DFN-A (CP 23) fired bursts of action potentials after the completion of the swimming pattern. This recording of the dorsal cerebral-pleural ganglion also contained a portion of the pedal ganglion (Pd 87, 88).

In four dorsal-side recordings, we found at least 7 DPN to be candidate swimming interneurons (Figs. 6 & 7, light blue). In one of these four recordings, 13 neurons with DPN activity were found, 6 of which fired at a low frequency. The DRI did not appear in our recordings, perhaps because of interference from the statocysts. One DPN also appeared near the cerebral-pleural border in our best ventral-side recording.

Seven VPN appeared along the fused border of the cerebral-pleural ganglion in one ventral-side recording (Fig. 8, light green). Due to relatively low firing frequency in two of these neurons, only five made good candidate swimming interneurons. Because none were in a position to be considered as a candidate VSI-B (see Getting PA, 1983 [13] for explanation of VSI subtypes), complete models of the swimming network should account for at least six different VPN in the cerebral-pleural ganglion (Table 1). VPN were also found on the dorsal side of the cerebral ganglion, including candidate VSI-A ([5]; Fig. 7).

Another unknown population of eight bursting neurons, not easily classified as either DPN or VPN, could be seen in one ventral-side recording (Fig. 8, orange). Signals from this population were faint suggesting that they may be below the outer surface of the ganglion. This recording indicates that the pattern-generating circuit in the swimming network may include groups of neurons that are active at times other than the two established phases (dorsal and ventral).

In two preparations, a large cerebral-ganglion neuron also fired rhythmic bursts of action potentials in phase with fictive swimming but only after skipping the first cycle (Fig. 8, pink). Other neurons in the cerebral-pleural ganglion fired only at the end of the fictive pattern or fired more strongly as the fictive swim progressed. The firing pattern of these neurons suggests that they could be involved in an active termination mechanism for the swimming response.

Another population of VPN found on the ventral side of the pleural ganglion fired at relatively low frequencies. A single large, weakly bursting neuron of this type also appeared in the pedal ganglion in one recording (Fig. 8, brown). Neurons of this type probably should not be considered as candidate swimming interneurons because previous work has shown that most large, weakly firing neurons in the pleural ganglion have an axon or dendrite in one or more nerves [4].

We estimated of the size of the DPN and VPN populations from our single best recording (Table 1). Adding the dorsal and ventral sides would give a less conservative estimate of 9 DPN and 8 VPN in each cerebral-pleural ganglion. Inclusion of the more slowly firing neurons would raise the estimate to about 15 DPN and about 15 VPN populations in each pair of cerebral-pleural ganglion.

Table 1: Population size estimates

Neuron Type	Previous Estimate*	Optical Recording
DFN-A	30	49
DFN-B	20	12
VFN	10	22
DPN	5	7
VPN	2	5

* From Hume RI & Getting PA, 1982 [6]; Getting PA, 1983 [1]

2.3. Other Patterns

In a few preparations, flexion neurons and candidate swimming interneurons fired in a coordinated manner distinct from the fictive swimming pattern (Fig. 9). Active populations in these alternate patterns included some but not all swimming-network neurons. These may be fictive

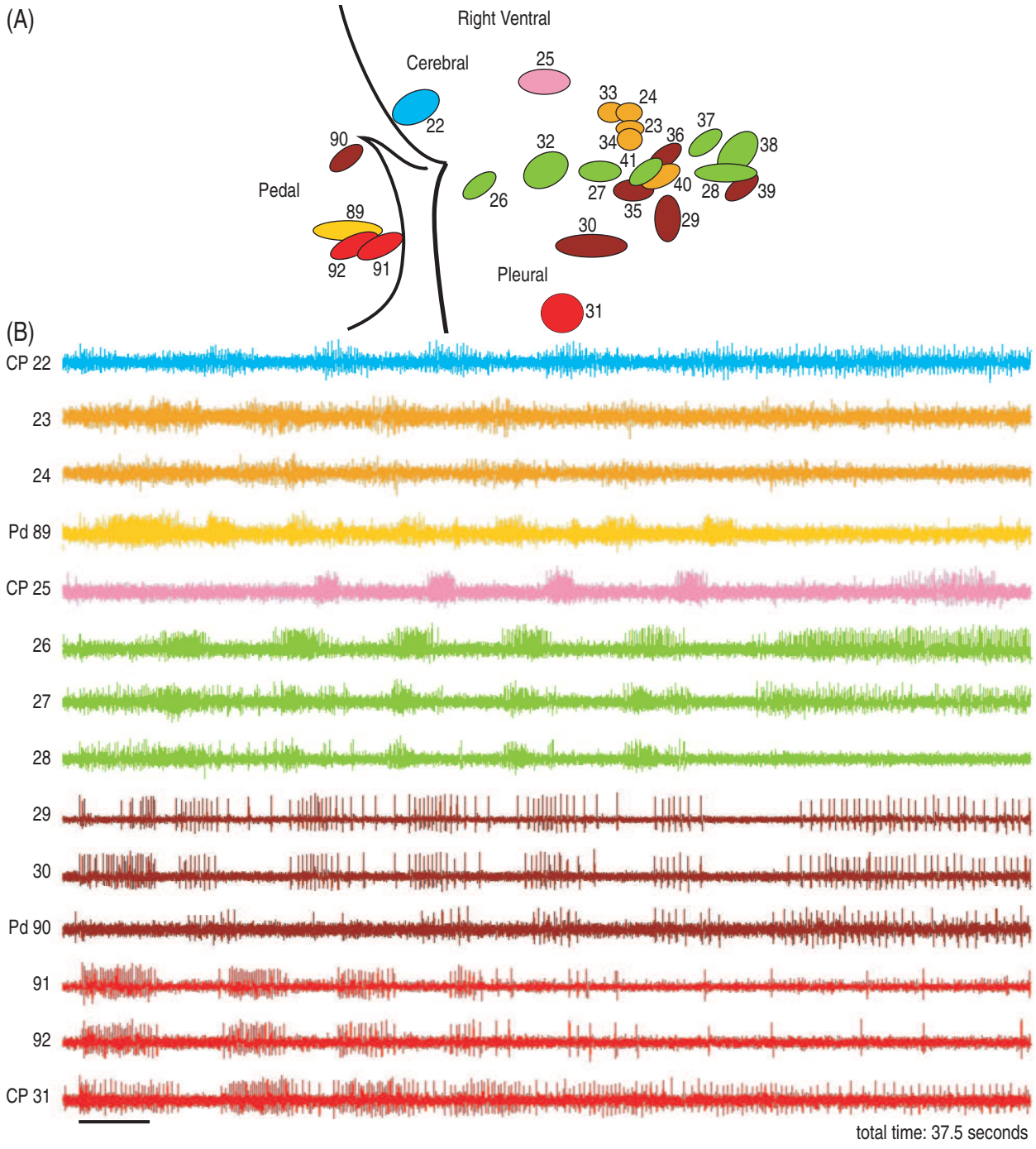

Figure 8: Ventral cerebral-pleural ganglion.
Place maps for seven VPN (examples in light green, CP 26-28) and one DPN (light blue, CP 22) were spread along the fused border between the cerebral and pleural ganglion on the ventral side. Five other neurons (orange, examples, CP 23, 24) were not easily classified as VPN or DPN. Another previously unidentified neuron (pink, CP 25) burst during the DPN phase of the cycle but did not fire on the first cycle of fictive swimming. Bursts from one pedal ganglion neuron (yellow, Pd 89) were not phase locked with the other neurons in the swimming network and fired more than one burst per cycle. An apparent DFN-A (CP 31) appeared in the pleural ganglion. Another group of relatively large neurons (brown, CP 29,39, Pd 90) fired low-frequency bursts out of phase with the DFN-A, and may be a new VFN subtype.

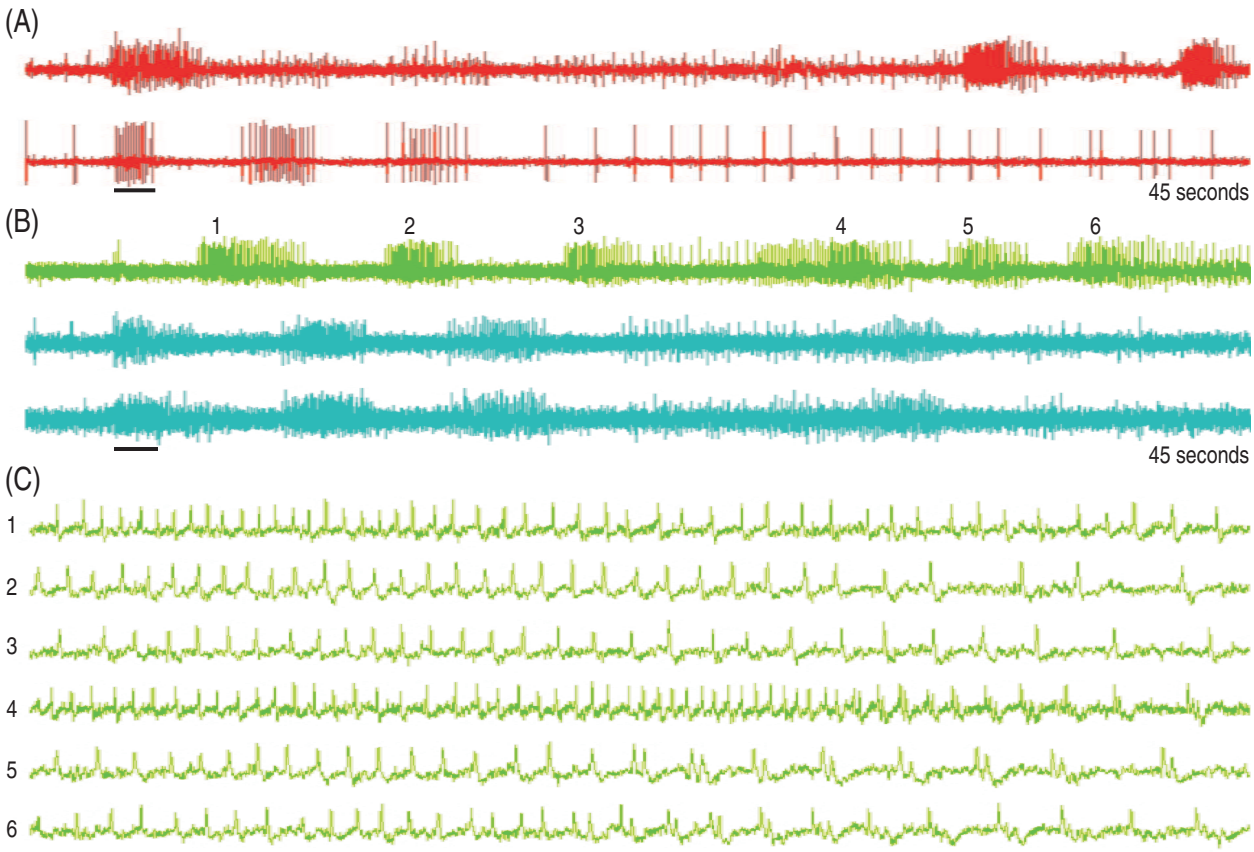

Figure 9: Multifunctional swimming network neurons.
(A) Multiple DFN-A firing modes. Two DFN-A were recorded from the dorsal side of the pedal ganglion during a two cycle fictive swimming episode. The top neuron appeared to participate in a second unknown pattern that was not swimming, and this bursting pattern was shared by some (not shown) but not all (lower trace) DFN-A in the ganglion.
(B) Multiple DSI firing modes. In another preparation (cerebral-pleural ganglion, dorsal aspect), a VPN (top) and two candidate DSI fired bursts of action potentials after fictive swimming terminated. The serotonergic DSI have at least three identified firing modes, and the pattern shown here may be a fourth [17, 18]. The six bursts in the top trace are expanded in (C) below.
(C) Three phase burst pattern. This VPN from (B) above had two phases per cycle during fictive swimming (top three traces), firing and not firing. The second pattern had three distinct phases, a burst of singlet spikes, a burst of doublet or triplet spikes, and not firing (bottom three traces).

motor patterns for behaviors like twisting that normally follow swimming, but more work will be necessary to determine whether or not these patterns correspond to actual behaviors.

3. Discussion

In this study we used Independent Components Analysis (ICA) to improve on previous techniques for isolating single neurons from optical recordings with voltage-sensitive dyes, bringing us closer to the goal of achieving a complete description of the neural activity during a behavior. A recent study of the medicinal leech using optical recordings with voltage sensitive dyes used Principal Component Analysis (PCA) to identify groups of neurons that participated in decision making after

single neurons were identified by other means [7]. Unlike ICA, which uses higher-order information in the statistics of the signals to perform blind source separation, PCA only uses the second-order covariance information in the signals [19]. PCA vectors are also constrained to be orthogonal but ICA vectors can in general be non-orthogonal, which is more flexible for analyzing mixtures.

Another way to monitor population activity is with multi-electrode arrays that isolate individual neurons, but the sample of neurons is sparse and incomplete [20, 21, 22]. Previous studies using voltage-sensitive dyes have monitored average patterns of activity in the chick auditory cortex [23], the slug olfactory system [24], the rabbit heart [25], and the human brain during epilepsy [26], but not individual neurons. Voltage-sensitive dye studies of individual neurons pioneered in the abdominal ganglion of Aplysia have shown that current models of the Aplysia gill-withdrawal reflex are incomplete [27, 28, 29]. They also indicate that network neurons participate in multiple behaviors [42] and that simple types of learning such as habituation and sensitization involve changes in large networks of neurons [30].

Tritonia flexion neurons are especially favorable for optical recording due to their relatively large size and their position on the surface of the pedal ganglion. Optical recording allowed us to simultaneously monitor a large fraction of the neurons in the pedal ganglion, free of assumptions about their locations. Although we fell short of recording all of the activity in the *Tritonia* brain, we substantially improved on what was previously known about the neurons participating in fictive swimming. We identified a total of 83 flexion neurons compared with previous estimates of 60 (Table 1). We also identified previously unknown types of pedal ganglion neurons (Fig. 5).

Candidate interneurons were designated Dorsal Phase Neurons (DPN) if they fired bursts of action potentials that overlapped with certain types of firing patterns (DFN or candidate DSI) or Ventral Phase Neurons (VPN) if their bursts did not overlap with bursts in these neurons. We found more candidate interneurons in the cerebral-pleural ganglion than had previously reported (Figs. 6, 7, 8; Table 1). Because there were more DPN and VPN than predicted by current models of the swimming network, we conclude that current models are incomplete. Additionally, we recorded neurons in the cerebral-pleural ganglion with previously unreported bursting patterns: a DPN candidate interneuron that skipped the first cycle (Figs. 8, 10, pink), a population of VPN that fired at relatively low frequencies (Figs. 8, 10, brown), and other bursting cells (Figs. 6, 7, 8, 10, orange). In Figure 10, we summarize the bursting patterns we found in the cerebral-pleural ganglion.

Some of these newly identified interneurons may participate in the oscillator itself where VPN and DPN are connected by reciprocal inhibition [1, 13]. Others, like C2, may have a different role in the oscillator. Still others may simply be connected to and follow the oscillator in order to perform swim-related tasks like coordinating flexion neurons or terminating the response. Further study, including determining their synaptic connectivity through intracellular recording and stimulation, will be required to determine their function.

Our recordings also contained tantalizing glimpses of patterned activity distinct from the fictive-swimming sequence (Fig. 9). Coordinated bursts of action-potential activity occurred in many network neurons after the end of fictive swimming in cases. A new bursting pattern was found in one candidate DSI, which may have implications for the role of serotonin in the *Tritonia* nervous system [17, 18]. We also observed doublets which have been attributed to near-threshold currents in *Tritonia* neurons. It would be of interest to determine how these currents are regulated during bursts of this type [16].

Future studies could help us establish firing patterns in the same network of neurons for different *Tritonia* behaviors [31] and record the neural correlates of learning in the *Tritonia* swimming network [32, 3, 33]. As voltage-sensitive dyes improve, recording synaptic potentials and even the

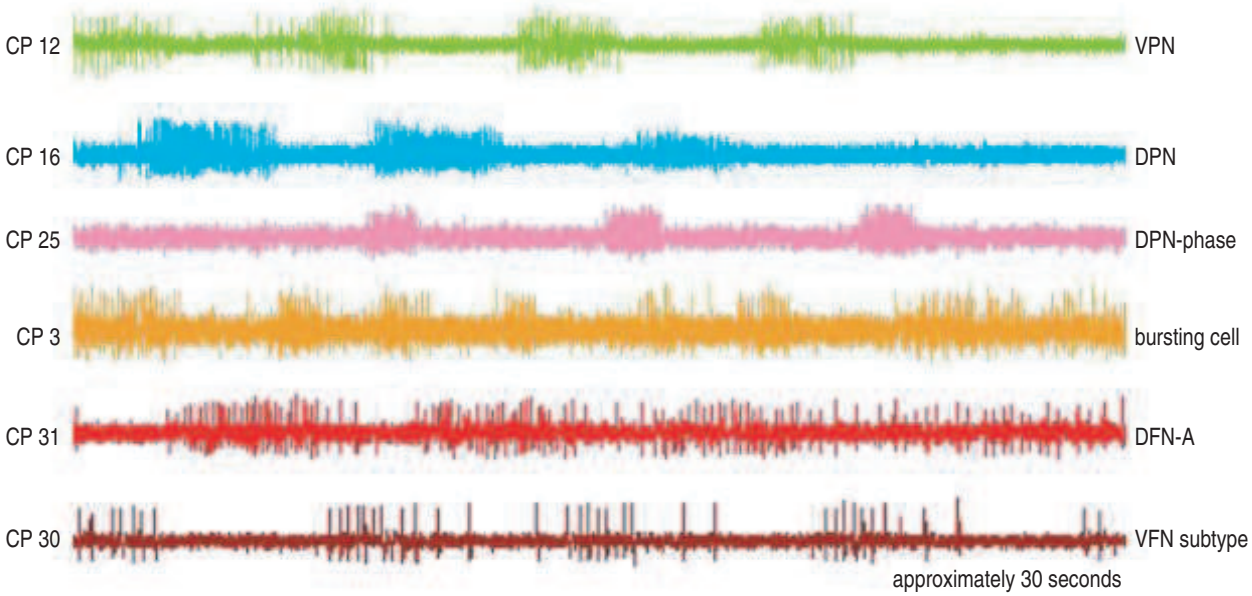

Figure 10: Summary of neuron types in the cerebral-pleural ganglion.
Composite figure of neuron types found in the cerebral-pleural ganglion, using traces from figures 6, 7, and 8. Traces begin just after the end of the stimulus. The traces were aligned and scaled relative to each other using common neuron types across recordings. Because of slight differences in cycle length across each recording, the alignment is only approximate but gives a sense of the relative timing and frequencies of bursts in different neuron types. The duration of the recording was approximately 30 sec.

membrane potential of each neuron may be possible [34, 35], which will be especially important for local networks that use graded membrane potential and not action potentials for synaptic communication [36].

Current models of the *Tritonia* swimming network ([1]; Fig. 1B) will need to be expanded to integrate all the neuron types and firing patterns reported here (Figs. 2, 5, 6, 7, 8, 10) and take into account the variability between neurons of a type (e.g. Figs. 3, 4). Data analysis methods like ICA (see Materials and Methods) will be invaluable for automating data processing and interpreting results [19, 21]. Synaptic wiring diagrams can be constrained by the observed patterns of action potential activity [37, 38].

Rhythmic behaviors such as respiration, feeding, and swimming may share cellular and synaptic mechanisms across species [31, 39]. Using appropriate physiological and computational techniques to decipher the *Tritonia* swimming network could help us understand the general design and operation of networks underlying all rhythmic behaviors.

4. Materials and Methods

4.1. Optical Recording

Tritonia were collected from several near-shore sites in the Puget Sound Region of the United States and shipped to Amagasaki, Japan in coolers. Slugs were maintained in artificial seawater at 10-12o C, and isolated brains were maintained at 11^{o}C during optical recordings [2]. The outer sheath around the ganglia and connective tissue were removed leaving the transparent inner sheath. An electrical stimulus (2.5 ms pulses for 3 s at 10 Hz, 100 μA) applied to right pedal nerve 3 reliably

activated previously identified neurons that burst at predictable times during the fictive swimming pattern [3, 4].

The isolated brain was bathed in the voltage-sensitive absorbance dye NK3041 (1.33 mg/ml; Nippon Kankoh Shikiso, Okayama, Japan) for 15-20 minutes and then returned to filtered seawater. The strongest optical signals were obtained from neurons in the plane of focus of the microscope. Neurons are distributed at different depths so we used several different views to try to ensure at least one high quality section through the dorsal and ventral regions of each ganglion. Our recordings centered on:

- only the Pedal ganglion
- primarily the Pedal ganglion with a portion of the Pleural ganglion
- the cerebral-pleural ganglion (the entirety of the ganglion did not fit into one recording)

The recorded populations of neurons within a given ganglion differed slightly because of different planes of focus between recordings. The depth of focus did not exceed the diameter of single large neurons. An intracellular recording electrode was used to monitor a flexion neuron during fictive swimming before, during, and after staining. Fictive swimming typically lasted between 3 and 7 cycles or about 20-40 seconds. A slight hyperpolarization of one to four millivolts was observed in many neurons during staining, and the spontaneous activity in the extracellular nerve recording also decreased during dye application.

Although prolonged exposure to the dye seemed to degrade the fictive swimming pattern somewhat, in both intracellular and extracellular recordings, no differences were observed to the fictive swimming pattern before and twenty minutes after staining. The membrane potential of individual neurons and the spontaneous activity in the nerve recording also appeared to recover after the brain was returned to filtered seawater.

Optical recording procedures have been described in detail previously [40, 41]. Action potentials appeared as a change in light absorbance at 705 ± 17 nm by a 448 element photodiode array with a 12x magnification on an upright microscope (each photodiode had a $76\mu m^2$ field of view). The objective magnification was 10x with a numerical aperture of 0.30. Each photodiode was amplified with an analogue amplifier and bandpass filtered with a low cutoff of 10 Hz and a high cutoff of 150 Hz. After this processing, each photodiode output was digitized at 1 KHz and stored on a computer hard drive.

We waited at least 30 minutes after staining and between trials before recording a fictive swimming sequence. The nerve stimulus used to elicit fictive swimming was applied four seconds after the onset of recording. A typical recording lasted 45 s, which was of sufficient duration to record the entire fictive swimming sequence in most cases. Neurons that fired rhythmic bursts of action potentials during fictive swimming were considered to be part of the swimming network.

Optical recording degraded the health of the brain as judged by the eventual failure of the nerve stimulus to produce a fictive swimming pattern. Recording was limited to at most 4 recordings or fictive swims per preparation. The most robust fictive patterns, including those used for data analysis here, occurred on the first or second trial in each preparation. Because previously identified neuron types fired in predictable ways, we were reassured that the swimming network was operating in a normal manner. However, shorter recording times or using a different dye might reduce photodynamic damage and allow for more trials in each preparation [42, 40, 43, 44].

4.2. Signal Processing

Each pixel in the diode array recorded a linear mixture of signals originating from an unknown number of neurons in addition to uncharacterized physiological and electronic artifacts. Automated spike train separation was performed using independent components analysis (ICA), a statistical signal processing technique that is effective when the sources are independent and not Gaussian [45]. We used infomax ICA [46, 47]. Briefly, we assume that the signals from the N photodiodes, $x = \{x_1(t), , x_N(t)\}$ are a linear mixture of the unknown sources, $s = \{s_1(t), , s_N(t)\}$,

$$x = As \tag{1}$$

where A is an unknown mixing matrix. In blind source separation the problem is to recover a version,

$$u = Wx \tag{2}$$

where u is identical to the original signals, s, except for scaling and permutation, by finding a square matrix, W, that linearly inverts the mixing process. The infomax ICA algorithm iteratively updates the unmixing matrix using the learning algorithm,

$$\Delta W = \alpha(I + f(u)u^T)W \tag{3}$$

where α is the learning rate, I is the identity matrix, ^{T} denotes transpose, and the vector-function, f, has elements,

$$f_i(u_i) = \frac{\delta}{\delta u_i} \ln g_i(u_i) \tag{4}$$

and the logistic sigmoid is given by,

$$g(u) = \frac{1}{1 + e^{-u}} \tag{5}$$

The number of sources (neurons and artifacts) that can be separated with ICA is no more than the number of mixtures (pixels). Because ICA does not recover sign or scale, no vertical scale bars appear with the spike trains reported here (Figs. 2, 3, 4, 5, 6, 7, 8, 9, 10). For further discussion on how infomax ICA is able to blindly separate neural signals and artifacts from optical recording data see Brown GD et al, 2001 [19].

ICA produced a continuous estimate of membrane potential for each neuron rather than a series of times or events. This allowed us to view actual spike shapes and even subthreshold membrane fluctuations in some neurons during the fictive pattern rather than more traditional raster display. ICA also allowed us to automatically separate individual neurons from recording artifacts as well as from each other. The high prevalence of synchronous spikes together with the proximity of neurons of a type made overlap resolution especially important in our study.

In addition to the time course of each membrane potential, ICA also provided topographic information. The location of each neuron on the detector array or place map was recovered from the ICA analysis, and these could be combined to make topographic maps (Figs. 2, 6, 7, 8). To these topographical maps we added outlines of the ganglia based on sketches and photographs made at the time of the recording and, in Ce-Pl recordings, the landmark provided by the statocyst. Prior knowledge about the localized nature of cell somata supported the validity of the ICA separation [19].

The number of operations done by the ICA algorithm increased as a fourth power of the number of detectors and linearly with the number of data points [47]. The ICA step took between a few minutes and a few hours depending on the amount of data and the speed of the computer processor.

For example, forty-five seconds of data from 100 detectors recorded at 1000 Hz were processed on a 1.6 GHz Pentium III computer in about 10 minutes. MATLAB (www.mathworks.com) software was used for all data analysis.

Removing detectors from the data set that did not appear to record any spiking activity reduced computer processing time and memory usage. This took only a few minutes using the conservative rule that if there was any doubt whether or not action potential activity was present on a given detector, that detector remained in the data set. A few detectors that did not appear to record spikes but did record shared artifacts also remained in the data set to facilitate the ICA analysis.

5. Acknowledgements

We thank Reiko Yamauchi and Hitomi Nishi for help with data analysis and Martina Wicklein for reading a draft of the manuscript. This work was supported by grants from the National Science Foundation, the National Institutes of Health and the Howard Hughes Medical Institute. MATLAB routines and complete optical recording data are available by request.

References

[1] P.A. Getting. Mechanisms of pattern generation underlying swimming in *Tritonia* II. network reconstruction. *J Neurophys*, 49, 1983.

[2] D.A. Dorsett, A.O. Willows, and G. Hoyle. The neuronal basis of behavior in *Tritonia*. iv. the central origin of a fixed action pattern demonstrated in the isolated brain. *J Neurobiol*, 4, 1973.

[3] G.D. Brown. Isolated-brain parallels to simple types of learning and memory in *Tritonia*. *Physiol & Behav*, 62, 1997.

[4] A.O. Willows, D.A. Dorsett, and G. Hoyle. The neuronal basis of behavior in *Tritonia*. i. functional organization of the central nervous system. *J Neurobiol*, 4, 1973.

[5] P.A. Getting. Neuronal organization of escape swimming in *Tritonia*. *J Comp Physiol*, 121, 1977.

[6] R.I. Hume and P.A. Getting. Motor organization of *Tritonia* swimming II. synaptic drive to flexion neurons from premotor interneurons. *J Neurophysiol*, 47, 1982.

[7] K.L. Briggman, H.D. Abarbanel, and W.B. Jr. Kristan. Optical imaging of neuronal populations during decision-making. *Science*, 307, 2005.

[8] G. Hoyle and A.O. Willows. Neuronal basis of behavior in *Tritonia*. II. relationship of muscular contraction to nerve impulse pattern. *J Neurobio*, 4, 1973.

[9] A.O. Willows, D.A. Dorsett, and G. Hoyle. The neuronal basis of behavior in *Tritonia*. iii. neuronal mechanism of a fixed action pattern. *J Neurobio*, 4, 1973.

[10] R.I. Hume, P.A. Getting, and M.A. Del Beccaro. Motor organization of *Tritonia* swimming. i. quantitative analysis of swim behavior and flexion neuron firing patterns. *J Neurophysiol*, 47, 1982.

[11] P.H. Taghert and A.O. Willows. Control of a fixed action pattern by single, central neurons in the marine mollusc, *Tritonia diomedea*. *J Comp Physiol*, 123, 1978.

[12] W.N. Frost and P.S. Katz. Single neuron control over a complex motor program. *Proc Nat Acad Sci USA*, 93, 1996.

[13] P.A. Getting. Mechanisms of pattern generation underlying swimming in *Tritonia* III. intrinsic and synaptic mechanisms for delayed excitation. *J Neurophys*, 49, 1983.

[14] P.A. Getting. Mechanisms of pattern generation underlying swimming in *Tritonia*. I. neuronal network formed by monosynaptic connections. *J Neurophys*, 46, 1981.

[15] R.W. Snow. Characterization of the synaptic actions of an interneuron in the central nervous system of *Tritonia*. *J Neurobiol*, 13, 1982.

[16] G.D. Brown and T.J. Sejnowski. Output sign switching in molluscan neurons is mediated by a novel voltage-dependent sodium current. In *Proceedings of the 4th Joint Symposium on Neural Computation.*, La Jolla, CA, 1997. Institute for Neural Computation, UCSD.

[17] A.D. McClellan, G.D. Brown, and P.A. Getting. Modulation of swimming in *Tritonia*, excitatory and inhibitory effects of serotonin. *J Comp Physiol*, 174, 1994.

[18] G.D. Brown. The role of serotonin in *Tritonia diomedea*. *American Zoologist*, 41, 2001.

[19] G.D. Brown, S. Yamada, and T.J. Sejnowski. Independent components analysis at the neural cocktail party. *Trends in Neuroscience*, 24, 2001.
[20] C.T. Nordhausen, E.M. Maynard, and R.A. Normann. Single unit recording capabilities of a 100 microelectrode array. *Brain Research*, 726, 1996.
[21] M. Laubach, J. Wessber, and M.A. Nicolelis. Cortical ensemble activity increasingly predicts behavior outcomes during learning of a motor task. *Nature*, 405, 2000.
[22] L.M Frank, E.N. Brown, and M. Wilson. Trajectory encoding in the hippocampus and entorhinal cortex. *Neuron*, 27, 2000.
[23] M. Asako, T. Doi, A. Matsumoto, S.M. Yang, and T. Yamashita. Spatial and temporal patterns of evoked neural activity from auditory nuclei in chick brainstem detected by optical recording. *Acta Otolaryngol*, 119, 1999.
[24] R. Gervais, D. Kleinfeld, K.R. Delaney, and A. Gelperin. Central and reflex neuronal responses elicited by odor in a terrestrial mollusk. *J Neurophysiol*, 76, 1996.
[25] J. Jalife. Spatial and temporal organization in ventricular fibrillation. *Trends in Cardiovascular Medicine*, 9, 1999.
[26] B. Albowitz, U. Kuhnt, R. Kohling, A. Lucke, H. Straub, E.J. Speckmann, I. Tuxhorn, P. Wolf, H. Pannek, and Oppel F. Spatio-temporal distribution of epileptiform activity in slices from human neocortex, recordings with voltage-sensitive dyes. *Epilepsy Research*, 32, 1998.
[27] S. Yamada, M. Nakashima, and S. Shiono. Reinforcement learning to train a cooperative network with both discrete and continuous output neurons. *IEEE Trans Neural Networks*, 9, 1998.
[28] D.W. Morton, H.J. Chiel, L.B. Cohen, and J.Y. Wu. Optical methods can be utilized to map the location and activity of putative motor neurons and interneurons during rhythmic patterns of activity in the buccal ganglion of aplysia. *Brain Research*, 564, 1992.
[29] Y. Tsau, J.Y. Wu, H.P. Hopp, L.B. Cohen, D. Schiminovich, and C.X. Falk. Distributed aspects of the response to siphon touch in aplysia, spread of stimulus information and cross-correlation analysis. *J Neurosci*, 14, 1994.
[42] J.Y. Wu, L.B. Cohen, and C.X. Falk. Neuronal activity during different behaviors in aplysia, a distributed organization? *Science*, 263, 1994.
[30] C. Hickie, L.B. Cohen, and P.M. Balaban. The synapse between le sensory neurons and gill motoneurons makes only a small contribution to the aplysia gill-withdrawal reflex. *European J of Neurosci*, 9, 1997.
[31] P.A. Getting and M.S. Dekin. *Tritonia* swimming, a model system for integration within rhythmic motor systems. In A.I. Selverston, editor, *Model Neural Networks and Behavior*, pages 3–19. Plenum Press, New York, 1985.
[32] G.D. Brown. Heterostimic enhancement of a not so fixed action pattern. *Netherlands Journal of Zoology*, 44, 1994.
[33] G.D. Brown. Nonassociative learning processes affecting swimming probability in the seaslug *Tritonia diomedea*, habituation, sensitization, and inhibition. *Behav Brain Res*, 95, 1998.
[34] M. Tanifuji, A. Yamanaka, R. Sunaba, S. Terakawa, and K. Toyama. Optical responses evoked by white matter stimulation in rat visual cortical slices and their relation to neural activities. *Brain Research*, 738, 1996.
[35] T.W. Cacciatore, P.D. Brodfuehrer, J.E. Gonzalez, T. Jiang, S.R. Adams, R.Y. Tsien, W.B. Jr Kristan, and Kleinfeld D. Identification of neural circuits by imaging coherent electrical activity with fret-based dyes. *Neuron*, 23:449–459, 1999.
[36] K. Graubard, J.A. Raper, and D.K. Hartline. Graded synaptic transmission between spiking neurons. *Proc Nat Acad Sci USA*, 77, 1980.
[37] S. Yamada, K. Matsumoto, M. Nakashima, and S. Shiono. Information theoretic analysis of action potential trains. ii. analysis of correlation among n neurons to deduce connection structure. *J Neurosci Methods*, 66, 1996.
[38] K. Oshio, S. Yamada, and M. Nakashima. Neuron classification based on temporal firing patterns by the dynamical analysis with changing time resolution (dct) method. *Biol Cybern*, 88, 2003.
[39] T.G. Brown. Intrinsic factors in the act of progression in the mammal. *Proc Royal Soc London*, 84, 1911.
[40] M. Nakashima, S. Yamada, S. Shiono, M. Maeda, and F. Satoh. 448-detector optical recording system, development and application to aplysia gill-withdrawal reflex. *IEEE Transactions on Biomedical Engineering*, 39, 1992.
[41] S. Yamada, H. Kage, M. Nakashima, S. Shiono, and M. Maeda. Data processing for multi-channel optical recording, action potential detection by neural network. *J Neurosci Meth*, 43, 1992.
[43] J.E. Gonzalez and R.Y. Tsien. Improved indicators of cell membrane potential that use fluorescence resonance energy transfer. *Chem Biol*, 4, 1977.
[44] B. Kuhn, P. Fromherz, and W. Denk. High sensitivity of stark-shift voltage-sensing dyes by one- or two-photon excitation near the red spectral edge. *Biophysical Journal*, 87, 2004.
[45] P. Comon. Independent component analysis, a new concept? *Signal Processing*, 36, 1994.
[46] A.J. Bell and T.J. Sejnowski. An information-maximization approach to blind separation and blind deconvolution. *Neural Computation*, 7, 1995.

[47] S. Amari, A. Cichocki, and Yang HA. A new learning algorithm for blind signal separation. *Advances in Neural Information Processing Systems*, 8, 1996.